

Sr₂V₃O₉ and Ba₂V₃O₉: quasi one-dimensional spin-systems with an anomalous low temperature susceptibility

E. E. Kaul¹, H. Rosner², V. Yushankhai¹, J. Sichelschmidt¹, R. V. Shpanchenko³
and C. Geibel¹

¹*Max Planck Institut für Chemische Physik fester Stoffe, Nöthnitzer Str. 40, 01187 Dresden, Germany*

²*Department of Physics, University of California, Shields Avenue, Davis, CA 95616, USA*

³*Department of Chemistry, Moscow State University, 199899 Moscow, Russia*
(November 15, 2018)

The magnetic behaviour of the low-dimensional Vanadium-oxides Sr₂V₃O₉ and Ba₂V₃O₉ was investigated by means of magnetic susceptibility and specific heat measurements. In both compounds, the results can be very well described by an $S = \frac{1}{2}$ Heisenberg antiferromagnetic chain with an *intrachain* exchange of $J = 82$ K and $J = 94$ K in Sr₂V₃O₉ and Ba₂V₃O₉, respectively. In Sr₂V₃O₉, antiferromagnetic ordering at $T_N = 5.3$ K indicate a weak *interchain* exchange of the order of $J_{\perp} \cong 2$ K. In contrast, no evidence for magnetic order was found in Ba₂V₃O₉ down to 0.5 K, pointing to an even smaller *interchain* coupling. In both compounds, we observe a pronounced Curie-like increase of $\chi(T)$ below 30 K, which we tentatively attribute to a staggered field effect induced by the applied magnetic field. Results of LDA calculations support the quasi one-dimensional character and indicate that in Sr₂V₃O₉, the magnetic chain is perpendicular to the structural one with the magnetic exchange being transferred through VO₄ tetrahedra.

PACS: 75.50.Ee, 75.40.Cx, 71.20.Ps

I. INTRODUCTION

The discovery of the first inorganic Spin-Peierls system CuGeO₃¹ has lead to a strong revival of interest for one-dimensional spin systems. The thorough investigation of this compound performed in the last years has revealed new unexpected phenomena, like e.g. the coexistence of an antiferromagnetic state with the Spin-Peierls state in slightly doped CuGeO₃², as well as the importance of frustration, i.e. antiferromagnetic exchange between second nearest neighbours³. Unfortunately, despite intensive research, no second inorganic Spin-Peierls System, or example for a frustrated spin-chain could be yet established. A further new topic which has emerged in this field in the past years is the effect of a *Dzialoshinskii-Moriya*^{4,5} (DM) interaction and of a staggered g-factor anisotropy in such a spin-chain system. Both theoretical and experimental studies indicate that they lead to a pronounced increase of the susceptibility at low temperatures and to the opening of a gap in the magnetic excitation spectra upon applying a magnetic field^{6,7,8}. However, there are presently only very few systems where this effect could be investigated.

Most of the recent studies on one dimensional systems have been carried out on compounds based on Cu⁺², where the magnetism originates from the $S = \frac{1}{2}$, one *d*-hole Cu⁺²-state. Thorough investigations of one-dimensional systems based on

the electron counterparts, i.e. V^{+4} or Ti^{+3} , are scarce. For most of them only preliminary susceptibility measurements, if at all, have been reported. This is surprising, since Vanadium-based ternary and quaternary oxides form a large number of compounds, many of them crystallizing in low dimensional structures^{9,10}. Complex Vanadium oxides have a very rich structural chemistry¹¹, since Vanadium can be coordinated in pyramidal, tetrahedral, or octahedral form (depending on the oxidation state), and these polyhedra can be joined in a large variety of ways^{12,13}. Therefore, it is possible to get interesting arrangements of magnetic cations, resulting in anomalous magnetic properties. Thus e.g., unusual magnetic behaviours were observed in the past years in a series of compounds^{14,15} (CaV_2O_5 ^{16,17}, $Ca(Sr)V_3O_7$ ^{18,19,20}, $Ca(Sr)V_4O_9$ ^{21,22,23}, $Pb_2V_5O_{12}$ ²⁴) where V^{+4} in pyramidal coordination forms plaquettes connected in one or two dimensions. The possibility to tune the Vanadium valence between +4 (one d electron) and +3 (two d electrons) allows the realization of both $S = \frac{1}{2}$ and $S = 1$ spin systems, where one expect the strongest quantum effects. Compounds with an intermediate valence-state, as for example α' - NaV_2O_5 ^{25,26}, allow to study the interplay between magnetic and charge degrees of freedom. For both V^{+4} and V^{+3} states, depending on the local configuration of the V-atoms, degenerated or nearly degenerated t_{2g} levels can be achieved leading to additional orbital degrees of freedom. Combining these degrees of freedom might lead to new interesting phenomena. Thus V-compounds were e.g. suggested to be the ideal candidates for systems with strong biquadratic interactions^{27,28,29}.

We have therefore started a more detailed study of low dimensional ternary and quaternary Vanadium oxides. We present here our investigation of the magnetic and thermodynamic properties of $Sr_2V_3O_9$ (SVO) and $Ba_2V_3O_9$ (BVO) and discuss our experimental results using several basic models and band structure calculations. Whereas in most of the low-dimensional vanadates investigated so far V^{+4} has a square pyramidal coordination, in these two compounds V^{+4} is located in an octahedral environment. As our results show, this has a profound influence on the magnetic properties.

II. STRUCTURES

SVO and BVO were first synthesized by Bouloux et al.³⁰. Despite the identical stoichiometry, they crystallize in different structures, which were first determined by J. Feldmann and Hk. Müller-Buschbaum^{31,32} and latter on confirmed by O. Mentre et al.³³ and A. C. Dhaussy et al.³⁴ (Fig. 1). Both structures present three different V-sites. Two of them show a tetrahedral oxygen-environment and can therefore be assigned to V^{+5} , whereas one site shows an octahedral environment and can therefore be assigned to V^{+4} . Thus, in contrast to the situation e.g. in NaV_2O_5 , there is a clear and complete V^{+4} - V^{+5} charge ordering. The VO_6 -octahedra form chains, which are arranged in a very different way in the two compounds. In SVO, the octahedra are linked together by a common corner, whereas in BVO, they are linked by a common edge. In SVO, two adjacent chains are connected by VO_4 -tetrahedra, leading to the formation of planes which are separated by Sr-ions. In contrast, there is no simple connection between adjacent chains in the Ba-based compound. Thus, BVO has a well defined one-dimensional structure whereas SVO seems to be more two-dimensional.

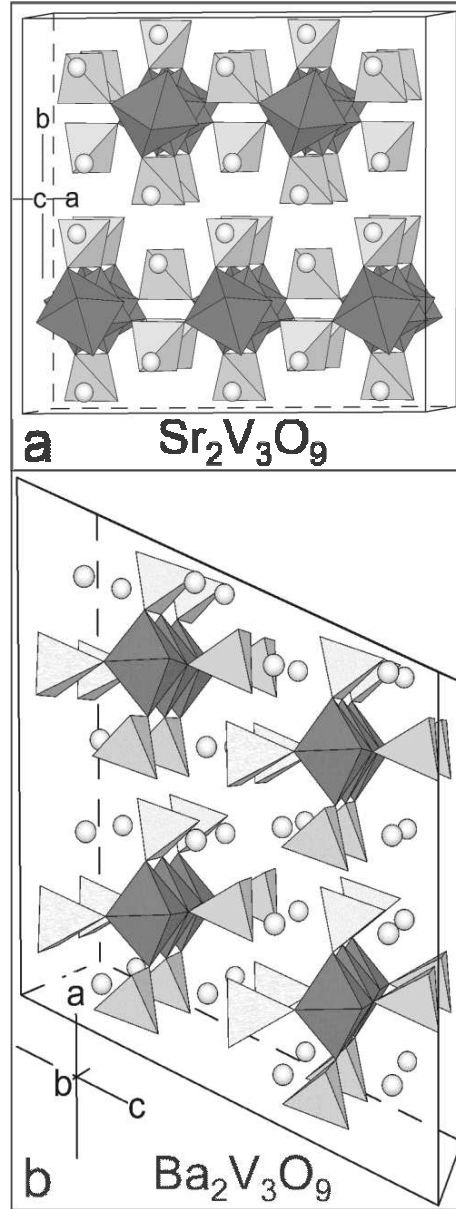


FIG. 1. View of the crystal structures of $\text{Sr}_2\text{V}_3\text{O}_9$ (a) and $\text{Ba}_2\text{V}_3\text{O}_9$ (b) along the structural VO_6 octahedra chains. In this figure the V^{+4}O_6 octahedra are dark grey, the V^{+5}O_4 tetrahedra are light grey and the Sr or Ba cations are shown as white spheres.

In both compounds, the VO_6 octahedra are slightly distorted, and the V^{+4} -ion is not located in the centre, but is slightly displaced by about 25 pm from the centre towards one of the O-ion (Fig. 2). This results in the formation of one short $V - O$ bond (the so called *vanadyl-bond*), with a $V - O$ distance $d \approx 0.17 \text{ nm}$, one opposite long $V - O$ bond, $d \approx 0.22 \text{ nm}$, and four equatorial bonds of similar, average length $d \approx 0.20 \text{ nm}$ towards the O-atoms forming the basal plane. The presence of the vanadyl bond determines clearly the *local axis* in each VO_6 octahedron. Normally the \hat{z} is taken parallel to this short bond. The direction of the

vanadyl-bond is suspected to be very important for the magnetic properties, since it determines which d orbital is occupied and therefore also determines the strength of the magnetic exchange along different directions. According to simple crystal field considerations, the off center displacement of the V-ion splits the t_{2g} triplet into a low lying d_{xy} -orbital singlet which is perpendicular to the vanadyl-bond and an excited orbital doublet (d_{xz} and d_{yz}).

In SVO, the vanadyl bond is formed between the V^{+4} and the O-ions that connects the octahedra but it is not clear in which sense it is directed. The refinement of the XR-data^{31,32} lead to a splitting of the V-site towards both directions, both positions being statistically occupied to 50%. From simple energy considerations, one expect a long range ordering of the vanadyl bonds within one chain, all pointing in the same sense, in order to avoid one connecting O-ion being involved into two vanadyl bonds (in this case the oxydation state of the Oxygen would be lower than -2). In contrast, correlation in the direction of the vanadyl bond between different chains might be absent because the difference in the total-energy between parallel and antiparallel arrangement should be extremely weak. Thus the entire structure of the 3D ground state remains unclear at present. In SVO the local axis of the octahedra are tilted from the direction of the chains by an angle of $\sim 17.5^\circ$ and alternates along the chain. This alternation leads to a staggered component of an anisotropic g-factor. At the same time, the occupied d -orbital would be almost perpendicular to the octahedra-chain. For that, one expect a very weak magnetic exchange along the structural chain, because there is no overlap between the occupied d -orbital and the p -orbitals of the connecting O-atoms. On the contrary, one expect a much stronger magnetic superexchange via the VO_4 -tetrahedron connecting two VO_6 octahedra in adjacent chains. This would result in *magnetic* spin-chains perpendicular to the structural octahedra-chains.

In BVO, with edge-sharing octahedra, the successive planes of occupied d-orbitals and the vanadyl bonds as its normal are arranged in a zig-zag manner along the structural chain direction with an angle of $\sim 46.5^\circ$ with respect to it. Whereas Feldmann and Müller-Buschbaum claims a complete ordering of the vanadyl bonds, all bonds pointing in the same sense³², Dhaussy et al.³⁴ suggests only ordering within each chain, all bonds pointing in the same sense within one chain, but without correlation among the vanadyl bond between different chains. For neighboring occupied d-orbitals a common edge O-ion provides a short superexchange path via the p orbital lying parallel to the intersection of the vanadium d-orbital planes. This leads to a significant magnetic exchange along the structural chain.

Only little is known about the physical properties of both compounds. O. Mentre et al.³³ and A.C. Dhaussy et al.³⁴ performed preliminary measurements of the magnetic susceptibility $\chi(T)$. From the maximum observed in $\chi(T)$ they concluded that antiferromagnetic ordering occurs at $T_N = 50 K$ and $T_N = 58 K$ in SVO and BVO, respectively. However, our results shall show that this maximum is not related to a broadened antiferromagnetic transition but to the onset of AF-correlations in the one-dimensional spin-chains.

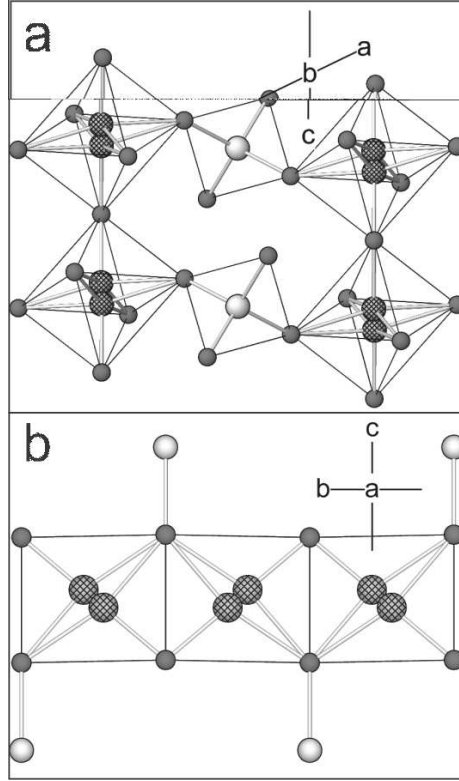


FIG. 2. Projection of the VO_6 -Octahedra perpendicular to the chains showing the splitting of the V-positions and how the octahedra are connected. a): $Sr_2V_3O_9$; b) $Ba_2V_3O_9$. In this figure the big checked circles are V^{+4} , the small dark grey ones are oxygen and the light grey ones are V^{+5} .

III. EXPERIMENTAL TECHNIQUES

Single phase polycrystalline samples of SVO and BVO were obtained by the method of solid state reaction in dynamical high vacuum. $A^{+2}V_3O_9$ ($A=\text{Sr, Ba}$) were synthesized from a stoichiometric mixture of $A_2V_2O_7$ and VO_2 at $900\text{ }^\circ\text{C}$ for 24 hs. $A_2V_2O_7$ were obtained heating a stoichiometric mixture of ACO_3 and V_2O_5 in air in two steps of 24hs. each one at 850 and $900\text{ }^\circ\text{C}$ respectively (with an intermediate ground). This preparation procedure lead to dark-red brown (SVO) and light-red brown (BVO) powder. Neither the crucible material (Al_2O_3 or Pt) nor the form of the starting mixture (intimately mixed powder or pressed pellet) had a significant influence on the results. The sample were characterized using a STOE powder-diffractometer. For both compounds, the diffractograms could be very well fitted using the structure proposed by Feldmann^{31,32}. No extra peaks corresponding to foreign phases were observed. The magnetic susceptibility $\chi(T)$ was measured between 2 and 400 K in fields up to 5 Tesla on powder samples in a commercial (Quantum Design) Squid. The specific heat (C_p) measurements were performed on pressed pellets with a relaxation method using a commercial PPMS equipment (Quantum Design). Measurements of the dielectric constants, which are reported elsewhere³⁵, show that both compounds are isolators.

IV. QUASI ONE-DIMENSIONAL MAGNETIC BEHAVIOUR

Despite the different crystallographic structures, the susceptibilities of both compounds are rather similar (Fig. 3). $\chi(T)$ follows a Curie-Weiss law at high temperatures, pass through a maximum around 50 K and 60 K for SVO and BVO, respectively, and increases again significantly below 30 K. In SVO, a well defined anomaly is seen at $T_N = 5.3$ K. The pronounced decrease of $\chi(T)$ below T_N points to a transition into an antiferromagnetic state. Since $\chi(T)$ has still a rather large value below T_N , a Spin-Peierls transition is unlikely. In contrast, no anomaly is observed for BVO down to 2 K. Preliminary ESR measurements show a $S = \frac{1}{2}$ spin susceptibility with a temperature dependence almost identical to that of the bulk susceptibility. The line shape observed in these measurements differs from a Lorentzian, as expected for low dimensional spin systems.

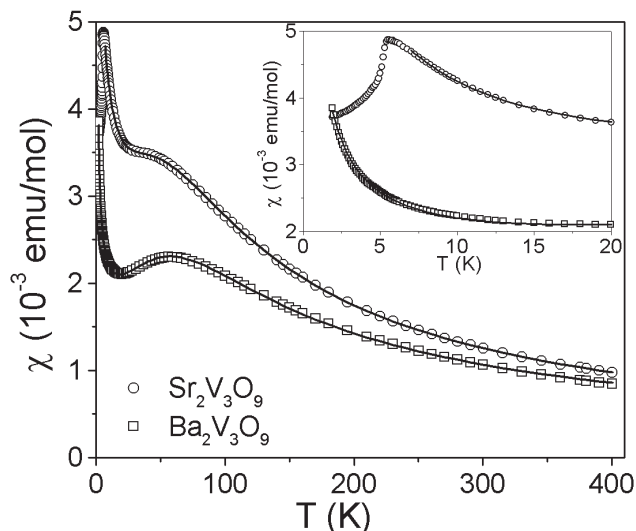


FIG. 3. Temperature dependence of the susceptibility of SVO (circles) and BVO (squares). The continuous lines show the fits of $\chi(T)$ using equation 1 as described in the text. Inset: susceptibility at low temperatures showing the antiferromagnetic transition at 5.3 K in SVO and the absence of transition in BVO.

The broad maximum in $\chi(T)$ is a hallmark for low dimensional spin systems, whereas the increase at low temperatures is rather unusual. We shall first focus on the low-dimensional behaviour and discuss the low-temperature increase latter on. We fit our susceptibility measurements with an expression of the form:

$$\chi(T) = \chi_{1D}(T) + \chi_{LT}(T) + \chi_{vv}(T) \quad (1)$$

$\chi_{1D}(T)$ is the contribution of the spin $S = \frac{1}{2}$ Heisenberg antiferromagnetic chains, which is known with a high precision over the whole measured temperature range³⁸. We took the polynomial approximation of Feyerherm⁸ (valid for $T > 0.05J/k_B$):

$$\chi_{1D}(T) = \frac{N_A \mu_{eff}^2}{3k_B T} \frac{1 + 0.08516x + 0.23351x^2}{1 + 0.73382x + 0.13696x^2 + 0.53568x^3} \quad (2)$$

with $x = \frac{|J|}{K_B T}$.

The increase at low temperatures was accounted for by a Curie-Weiss term, χ_{LT}

$$\chi_{LT}(T) = \frac{C}{T + \theta} \quad (3)$$

and we included a temperature-independent Van-Vleck contribution χ_{vv} .

With this approach, the experimental data could be fitted very nicely in the range $7 K < T < 400 K$ for SVO and $2 K < T < 400 K$ for BVO, respectively. The fits are shown as solid lines in Fig. 3 and the fits parameters are given in Table I. The effective moments of $\mu_{eff} = 1,79 \mu_B$ (SVO) and $\mu_{eff} = 1,64 \mu_B$ (BVO) obtained with these fits are close to the spin-only value expected for V^{+4} ions ($\mu_{eff} = 1,73 \mu_B$).

The quality of the fits supports the picture of an antiferromagnetic chain for both compounds. The values for the magnetic in-chain exchange J we got from these fits, $J \cong 82 K$ and $J \cong 94 K$ for SVO and BVO, respectively, are similar to that obtained in other V^{+4} compounds. However, the susceptibility is not very sensitive for discerning a $1D$ from a $2D$ spin-system since the temperature dependence of $\chi(T)$ is quite similar for a $S = \frac{1}{2}$ chain and for a $S = \frac{1}{2}$ square lattice, and differences in the absolute values can be accounted by changes in μ_{eff} . On the contrary, profound differences are expected in the magnetic part of the specific heat at low temperatures. For a $S = \frac{1}{2}$ chain, one expect a linear term, whereas for a square lattice, one expect a leading quadratic term. Thus more insight can be gained from the analysis of the specific heat.

	SVO	BVO
$T_N(K)$	5.3	<0.5
$J(K)$	82	94
$\chi_{vv}(emu/mol)$	2×10^{-5}	1×10^{-4}
$\theta(K)$	-4.5	-0.35
$C(emuK/mol)$	2.9×10^{-2}	4.8×10^{-3}
$\mu_{eff}(\mu_B)$	1.79	1.64

TABLE I. Parameters from the fits of the susceptibility for SVO and BVO shown in Fig. 3

The results of the specific heat measurements in the temperature range $0.5 K < T < 10 K$ are shown for both compounds in Fig. 4 as C_p/T versus T^2 -plots, in order to separate the different contributions. In both compounds, these plots follow a straight line over a considerable temperature range, from T_N to $15 K$ in SVO and from $2.5 K$ to $6 K$ in BVO indicating that $C_p(T)$ is the sum of a linear and a cubic contribution. Since the cubic term corresponds to the expected contribution of the phonons, this demonstrate that the leading term of the magnetic contribution in the unordered state (above T_N for SVO) is linear in T. For a $S = \frac{1}{2}$ antiferromagnetic Heisenberg-chain, theoretical calculations^{36,37} predict for low temperatures ($T < 0.2J$):

$$\frac{C_p}{T} = \frac{2Rk_B}{3J} = \gamma_{theor} \quad (4)$$

With the J -values obtained from the fit of $\chi(T)$, this correspond to predicted values $\gamma_{theor} = 68 \text{ mJ/K}^2\text{mol}$ (SVO) and $\gamma_{theor} = 59 \text{ mJ/K}^2\text{mol}$ (BVO). Fitting the specific heat data with:

$$C_p(T) = \gamma T + \beta T^3 \quad (5)$$

in the range $9 \text{ K} < T < 16 \text{ K}$ for SVO and $2.5 \text{ K} < T < 5 \text{ K}$ for BVO, we obtained $\gamma = 66 \text{ mJ/K}^2\text{mol}$ (SVO) and $\gamma = 59 \text{ mJ/K}^2\text{mol}$ (BVO), very close to the values predicted from the susceptibility results. This excellent agreement is a strong support for the quasi one-dimensional nature of the spin system in both compounds. In contrast, an attempt to explain the specific heat data with a square lattice completely failed, as shall now be demonstrated for SVO. For a two dimensional $S = \frac{1}{2}$ square array, the leading term in the magnetic specific heat is expected to be quadratic. We used the estimation of Takahashi³⁹:

$$C_p(T) = \delta T^2 = R \frac{3\zeta(3)}{4\pi J_{2D}^2 m_1^2} T^2 \quad (6)$$

with R the Gas constant, $\zeta(3) = 1.202$ and $m_1 = 1/2 + 0.078974$. J_{2D} can be estimated from the temperature of the maximum in $\chi(T)$, $T_{\chi_{max}}$, since theoretical calculations predict $T_{\chi_{max}} = 0.94 J_{2D}$. For SVO, this lead to $J_{2D} = 56.5 \text{ K}$ and thus $\delta = 2.2 \times 10^{-3} \text{ J/K}^3\text{mol}$. By adding the phonon contribution obtained from the T^3 term in the plot C_p/T versus T^2 ($\beta = 9.8 \times 10^{-4} \text{ J/K}^3\text{mol}$), we get the total specific heat shown by the dashed lines in Fig. 4. At low temperatures, the calculated specific heat is far below the experimental one, showing that even SVO is far from being a square lattice. Thus the observation of a large linear contribution in $C_p(T)$ at low temperatures, which matches very well with that expected taking the J -values obtained from the susceptibilities, is a very strong evidence that the magnetic coupling in both compounds is predominantly one dimensional and that the inter-chain coupling is weak. This inter-chain coupling J_{\perp} can be estimated from the ordering temperature, since in weakly coupled Heisenberg antiferromagnetic chains, T_N is determined by J_{\perp} . The exact relation is not known, but there exist a few theoretical predictions. A relation which has been frequently used and found to be quite reliable is that proposed by Schultz⁴⁰ for an isotropic interchain coupling J_{\perp} :

$$|J_{\perp}| = \frac{T_N}{4A \ln \sqrt{\left(\frac{\Lambda J}{T_N}\right)}} \quad (7)$$

with $A = 0.32$ and $\Lambda \cong 5.8$. Using our experimental results $T_N = 5.3 \text{ K}$ and $J = 82 \text{ K}$ for SVO, we obtain $J_{\perp} \cong 1.9 \text{ K}$. For BVO, $T_N < 0.5 \text{ K}$ leads to $J_{\perp} < 0.15 \text{ K}$. Thus the ratio between *intra*- and *inter*-chain coupling is 2.3×10^{-2} in SVO and below 1.6×10^{-3} in BVO, showing that both compounds are quasi one-dimensional spin-systems.

The specific heat of SVO shows at T_N a small, but well defined anomaly. Further on, there is a pronounced change in the T dependence of $C_p(T)$ from above to below T_N . Below T_N , the temperature dependence of $C_p(T)$ is dominated by a large cubic term, which can be attributed to 3-dimensional magnons in the antiferromagnetically ordered state. The weakness of the $C_p(T)$ anomaly at T_N in SVO is probably related to the small $\frac{T_N}{J}$ ratio. At these low temperatures (compared

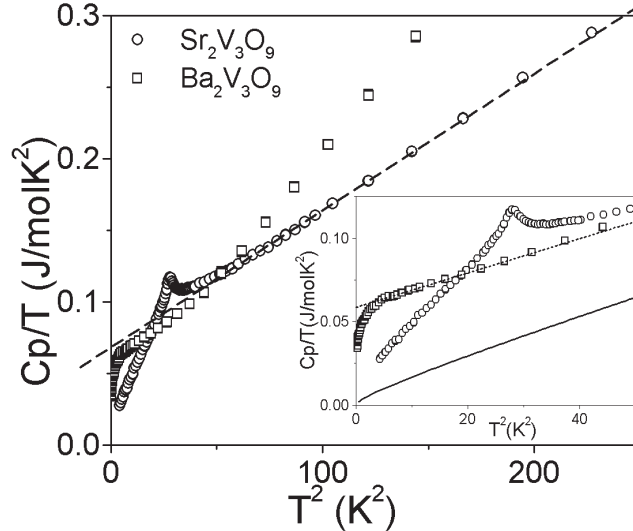


FIG. 4. Specific heat of SVO (Circles) and BVO (squares) plotted as $C(T)/T$ versus T^2 . Inset: specific heat at low temperatures. The dashed and the dotted lines show the fit $C(T) = \gamma T + \beta T^3$ as described in the text for SVO and BVO, respectively. The solid line in the inset indicate the result expected for SVO using a $S=1/2$ square lattice antiferromagnet model.

to J), quantum fluctuations are very strong in quasi one-dimensional spin-systems, reducing the size of the antiferromagnetically ordered moment and accordingly the size of the specific heat anomaly. Preliminary measurements under magnetic field indicate a broadening of this anomaly and a small shift to lower temperatures in fields of a few Tesla. Thus the $C_p(T)$ results confirm an antiferromagnetic phase transition at $T_N = 5.3$ K in SVO. In contrast, no anomaly was seen in the $C_p(T)$ of BVO down to 0.5 K, although the slope also increases towards low temperatures. The origin of this decrease is not clear yet.

V. LOW TEMPERATURE $\chi(T)$ UPTURN AND ANNEALING EFFECTS

We now turn to the Curie-like upturn of $\chi(T)$ at low temperatures (LT-CW). Usually, such an upturn is attributed to paramagnetic moments due to impurities or defects in the sample. However, it was recently demonstrated that such upturn can also be intrinsic. In quasi one-dimensional $S = \frac{1}{2}$ systems it arises due to the staggered field induced by the applied field^{6,7,8}. The DM interaction and a staggered g-factor anisotropy are two sources for the staggered field effect. A first indication for the intrinsic nature of the LT-CW in our compounds is given by the behaviour of $\chi(T)$ well below T_N in SVO. If the LT-CW would be due to paramagnetic impurities, it should also be present below T_N . However, below T_N , $\chi(T)$ decreases down to the lowest measured temperature of 1.9 K, without any trace of paramagnetic impurity contribution.

In an attempt to get more insight into this phenomena, we investigated the influence of different sample preparation conditions. We found that in BVO, $\chi(T)$ was almost insensitive to annealing, whereas in SVO, both the upturn in $\chi(T)$ and

the antiferromagnetic ordering presented a clear and systematic dependence on the annealing process. In Fig. 5, we show the evolution of $\chi(T)$ of a SVO sample after successive annealing steps at about 900 °C for 24 hrs in dynamical vacuum. Whereas the changes at higher temperatures are rather weak, pronounced differences are observed at low temperatures. The Curie-like upturn is always present, but its magnitude increases with the number of annealing steps. Further on, a strong shift of the transition temperature from $T_N = 2.4$ K in the *as grown* sample up to 5.3 K after the third annealing step is observed. Further annealing did not increase T_N any more suggesting that we reached saturation of T_N . In order to perform a quantitative analysis, the $\chi(T)$ curves were fitted using Eq. (1) and the effective moment μ_{LT} connected with the LT-CW was calculated from the coefficient C . All fit parameters for the three curves of Fig. 5 are given in Table II. μ_{LT} increases by a factor of 2 when T_N shifts from 2.4 K to 5.3 K, whereas J does not change appreciably and the high temperature effective moment increases only slightly. Interestingly, we found an excellent but intriguing correlation between T_N and the μ_{LT} , not only in this sample, but also in all investigated SVO samples. This correlation is demonstrated in Fig. 6, where we plot T_N versus μ_{LT} using all investigated samples. All points lie almost on one line. Presently the origin of this linear relation is not clear. However, μ_{LT} increasing with T_N is a further support that the LT-CW is not induced by defects. Defects are expected to weaken a coherent three-dimensional magnetic coupling and thus to reduce T_N . One would therefore expect a reduction of a defect induced LT-CW with increasing T_N which is opposite to what is observed. A high T_N implies a well defined magnetic coupling between adjacent chains and hence one can suspect that this requires a long range three dimensional order of the Vanadyl-bonds. This is supported by the observation that high T_N s were observed in those samples which were annealed as close as possible to the melting point, which is slightly above 900 °C. Since the ordering of the vanadyl-bonds between different chains involve not the independent flip of single V-atoms, but the coherent rearrangement of all the V-atoms within one octahedra-chain, one expect that this ordering can only take place very close to the melting point. Unfortunately, an attempt to determine changes in the ordering of the vanadyl bonds using Rietveld refinements of powder X-Ray patterns failed, because the superstructure reflexes connected with this order are too weak to be seen in powder patterns. These refinements showed some weak differences in the structure, but it was impossible to get a significant information about the ordering of the vanadyl bonds. One cannot exclude that some oxygen vacancies arise during subsequential annealings. However, from our point of view it looks unlikely since all oxygen atoms are connected either with vanadium V^{+5} forming stable VO^{-4} groups or involved in the formation of vanadyl bonds.

A correlation between a larger T_N and a larger inter-chain coupling can also be deduced from the specific heat. The specific heat at low temperatures of the three sample whose susceptibility was shown in Fig. 5 is plotted as C_p/T versus T^2 in Fig. 7. The magnitude of the linear term related to the one-dimensional spin-fluctuations is almost the same in all samples, in accordance with the sample independent J -value extracted from the analysis of $\chi(T)$ (Table II). This indicates that the intra-chain magnetic exchange is not affected by the annealing process. However, the temperature range where one can observe this linear term extends to lower temperatures with decreasing T_N . This also shows that the spin-fluctuations

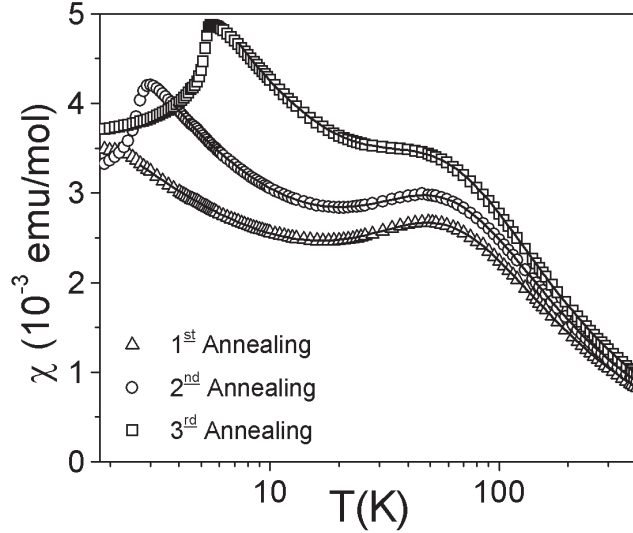


FIG. 5. Susceptibility of SVO after successive annealing. The continuous lines show the fits of $\chi(T)$ using equation 1 as described in the text.

remains one-dimensional down to lower temperatures, i.e that the inter-chain exchange is decreasing, in accordance with the decrease of T_N . The absence of an upturn of $C_p(T)$ at low temperatures is an indication for the absence of paramagnetic defects. One expect that a residual magnetic coupling of the defects to the lattice should slightly lift the degeneracy of the magnetic state of the defect and thus lead to a Shottky-like increase of $C_p(T)$ towards low temperatures.

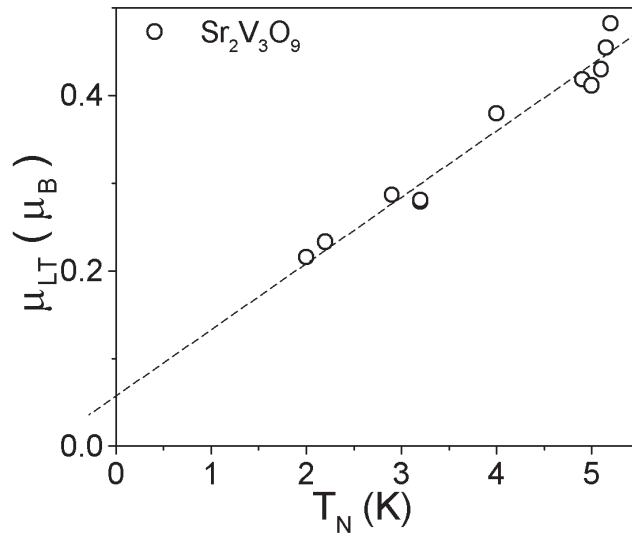


FIG. 6. Correlation between the transition temperature into the antiferromagnetic state T_N and the effective moment μ_{LT} connected with the low temperature increase in $\chi(T)$ in SVO.

Thus, the analysis of the experimental results rules out that paramagnetic defects are responsible for the increase of $\chi(T)$ at low temperatures. Therefore, we have to discuss possible intrinsic origins. The first trivial idea, that this upturn is due to

	1 st Annealing	2 nd Annealing	3 rd Annealing
$T_N(K)$	2.3	3	5.3
$J(K)$	81.3	80.8	82.2
$\chi_{vv}(emu/mol)$	5×10^{-5}	5×10^{-5}	2×10^{-5}
$\theta(K)$	-2.3	-1.5	-4.5
$C(emuK/mol)$	7.0×10^{-3}	1.01×10^{-2}	2.9×10^{-2}
$\mu_{eff}(\mu_B)$	1.65	1.73	1.79

TABLE II. Parameters from the fits of the susceptibility of SVO shown in Fig. 5

a weak ferromagnetic inter-chain interaction seems to be incorrect. The inclusion of a weak ferromagnetic inter-chain coupling within a mean field approach lead to a T-independent downwards shift of the $1/\chi(T)$ vs T curve, i.e to a larger increase of $\chi(T)$ at $T_{\chi_{max}}$ than below $T_{\chi_{max}}$, in contradiction to the experimental results. As stated above, the staggered field effect caused by the DM-interaction and the staggered g-factor anisotropy ($g_s \sim \pm(g_{\parallel} - g_{\perp})$) was recently demonstrated to be responsible for such upturn in some one-dimensional Cu^{+2} compounds^{6,8} and in Yb_4As_3 ⁷. Since our results are similar to the behaviour found in these systems, the staggered field effect appears to be a promising alternative explanation for our observations. According to Moriya⁵, a DM-interaction is expected if the mid-point between two interacting magnetic ions is not an inversion centre. Due to the low symmetry of our compounds, this condition is fulfilled in both SVO and BVO.

Standard rules predicts the intensity of the DM interaction to be proportional to $(\lambda/\Delta)J$, where λ is the strength of the spin-orbit interaction and Δ is the crystal field splitting of d-orbitals. One has $\lambda_V \simeq 0.03$ eV for V^{+4} as compared to $\lambda_{Cu} \simeq 0.1$ eV for Cu^{+2} . At the same time, the splitting of the t_{2g} orbital levels due to the off-center displacement of the V-ions ($\delta \simeq 0.2$ Å) was estimated by us to give $\Delta_V \simeq 0.2$ to 0.5 eV. In comparison, for Cu^{+2} normally $\Delta_{Cu} \simeq 1$ to 2 eV. Preliminary ESR measurements performed in SVO⁴¹ indicate a rather small g-factor anisotropy with $g_s \sim 10^{-2}$. Therefore, one can expect that in the Cu-compounds⁸, where the DM interaction and the g_s contribution are nearly equally operative, the resulting staggered field effect is somewhat stronger than that in the V-compounds under consideration. Contrary, the low temperature Curie constants C measured in BVO and, specially in SVO are even larger than the averaged one inferred from the data reported for the Cu compounds. We remind, however, that in Cu-benzoate⁴² the anomalous low temperature term χ_{LT} in $\chi(T)$ is also several times larger than that predicted in the theory⁶.

With the DM-interaction as origin of the $\chi(T)$ upturn, the difference between the annealing effects in SVO and BVO can be understood. As stated above, annealing should mostly affect the relative orientation of the vanadyl bond between adjacent (structural) V^{+4} -chains. Since in BVO, the structural V^{+4} chain and the magnetic chain are identical, a change of the orientation of the vanadyl bond between adjacent chains shall not affect the magnetic interaction along the magnetic chain. In SVO on the contrary, since the magnetic and the structural chains are orthogonal, a change of the orientation of the vanadyl bond between adjacent structural chains shall change the symmetry between adjacent V^{+4} ions along the magnetic chain and thus should directly affect the strength of the DM-interaction.

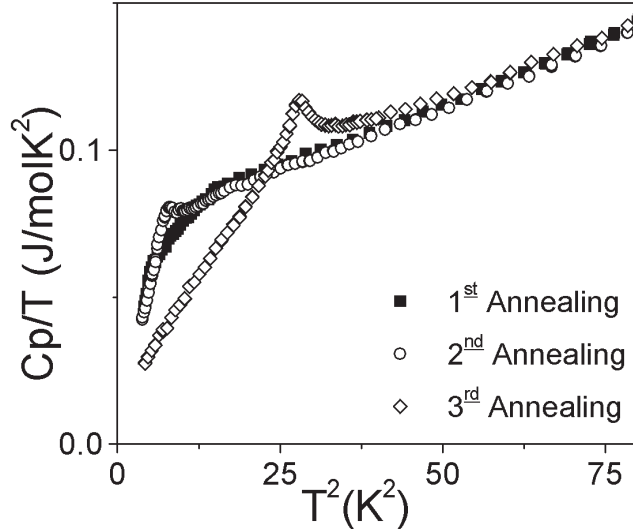


FIG. 7. Specific heat of SVO after successive annealing. The samples used are the same than in figure 5.

VI. BAND STRUCTURE CALCULATIONS

In order to get a better understanding and a consistent picture of the properties of SVO and BVO, we performed electronic structure calculations using the full-potential nonorthogonal local-orbital minimum-basis scheme⁴³ within the local density approximation (LDA). In the scalar relativistic calculations we used the exchange and correlation potential of Perdew and Zunger⁴⁴. $V(3s,3p,4s, 4p, 3d)$, $O(2s, 2p, 3d)$, $Sr(4s, 4p, 5s, 5p, 4d)$ and $Ba(5s, 5p, 6s, 6p, 5d)$ states, respectively, were chosen as the basis set. All lower lying states were treated as core states. The inclusion of $V(3s,3p)$ and $Sr(4s, 4p)$ as well as $Ba(5s, 5p)$ orbitals in the valence states was necessary to account for non-negligible core-core overlaps. The O $3d$ states were taken into account to increase the completeness of the basis set. The spatial extension of the basis orbitals, controlled by a confining potential⁴⁵ $(r/r_0)^4$, was optimized to minimize the total energy.

For the sake of simplicity, for SVO, a crystal structure with vanadyl bonds correlated between different chains (in phase) was calculated using the space group $C1c1$ (No. 9). We assume that the influence of the interchain correlation is of minor importance. The paramagnetic calculations result in the total density of states (DOS) and the partial DOS shown in the upper panel of Fig. 8. We find a valence band complex of about 7 eV width with two bands crossing the Fermi level corresponding to the two formula units per unit cell. Typical of vanadates, the valence band has mainly O $2p$ character, with some admixture of V and small contributions from Sr (not shown). The states at and right above the Fermi level are built primarily from V $3d$ orbitals, with the dispersion arising from hybridization with the O $2p$ states, with practically negligible admixture of Sr states. In the partial DOS, we can clearly distinguish between the two different types of V sites. The tetrahedrally coordinated V(1) and V(2) have only a very small contribution at the Fermi level. Disregarding the spread overlap charge with the O $2p$ valence states, this leads to a

picture of V^{+5} ions. On the other hand, the octahedral V(3) site shows a half filled orbital at the Fermi level, leading to a magnetically active spin $1/2 V^{+4}$ ion. Thus, the calculation is fully consistent with the empirical assignment of the different V species mentioned earlier.

Analyzing the Slater-Koster-Integrals for the different V(3)-O terms we find a much larger overlap for the short V(3)-O vanadyl bond compared with the longer V(3)-O bond to the opposite corner of the octahedron. Therefore, the electronic hopping along the octahedron chain is suppressed. This can be clearly seen in the band structure shown in the lower panel of Fig. 8. The dispersion along the “structural” chain direction ΓZ is rather weak and only about $1/3$ of the dispersion perpendicular to the “magnetic” chain along the ΓX direction (corresponding to the crystallographic a direction). This fully confirms the conjecture based on an empirical bond and orbital analysis made in section II. From the viewpoint of the electronic structure, a picture of VO_5 pyramids stacked along the c axis seems more appropriate than the picture of linked VO_6 octahedra. The dispersion in the third direction is extremely small, leading therefore to spatially very anisotropic exchange interactions for this compound.

In order to get a rough estimate for the exchange integrals, we analyze a tight binding (TB) model taking into account as a first approximation nearest neighbors (NN) only in each direction. Taking the monoclinic angle into account, this results in $t_a \sim 110$ meV, $t_c \sim 30$ meV and $t_b < 1$ meV. Here, t_a corresponds to the dispersion parallel to the “magnetic chain” running perpendicular to the c direction of the “structural” chain (compare Fig. 2a). These transfer integrals enable us to estimate the relevant exchange couplings, crucial for the derivation and examination of magnetic model Hamiltonians of the spin- $1/2$ Heisenberg type. In general, the total exchange J can be divided into an antiferromagnetic and a ferromagnetic contribution $J = J^{AFM} + J^{FM}$. In the strongly correlated limit, valid for typical vanadates, the former can be calculated in terms of the one-band extended Hubbard model $J_i^{AFM} = 4t_i^2/(U_{eff})$. The index i corresponds to NN in different directions, U_{eff} is the effective on-site Coulomb repulsion. Considering the fact that the VO_5 pyramids are not directly connected, but only via VO_4 tetrahedra, ferromagnetic contributions J^{FM} along the “magnetic” chain are expected to be small and we neglect them.⁴⁶ From LDA-DMFT(QMC) studies⁴⁷, by fitting spectroscopic data to model calculations⁴⁸ and similar LDA based model calculations⁴⁹, $U \sim 4-5$ eV is estimated for typical vanadates. In rough approximation, this leads to exchange integrals of $J_a \sim 110$ K, $J_c \sim 10$ K and $J_b < 0.1$ mK. With respect to the crude approximations made, the estimate for the leading exchange integral J_a is in surprisingly good agreement with the result $J_a = 82$ K from the fit to the susceptibility data. At first glance, the deviation from the experimentally estimated interchain exchange $J_{\perp} = 1.9$ K looks rather large, therefore this problem will be discussed more detailed in the following.

The (spatially) very anisotropic exchange interactions resembles strongly the situation in the straight corner shared cuprate chains Sr_2CuO_3 and Ca_2CuO_3 . These quasi 1D cuprate compounds exhibit antiferromagnetic intrachain exchange integrals J_{\parallel} of the order of 2000 K, but they order antiferromagnetically at $T_N \approx 5$ K and $T_N \approx 9$ K only,⁵⁰⁻⁵² respectively, due to the very weak interchain coupling. As in SVO, in those systems the coupling in the weakest direction is negligibly small and will be dominated even by the dipolar interactions. It has been shown⁵³ that

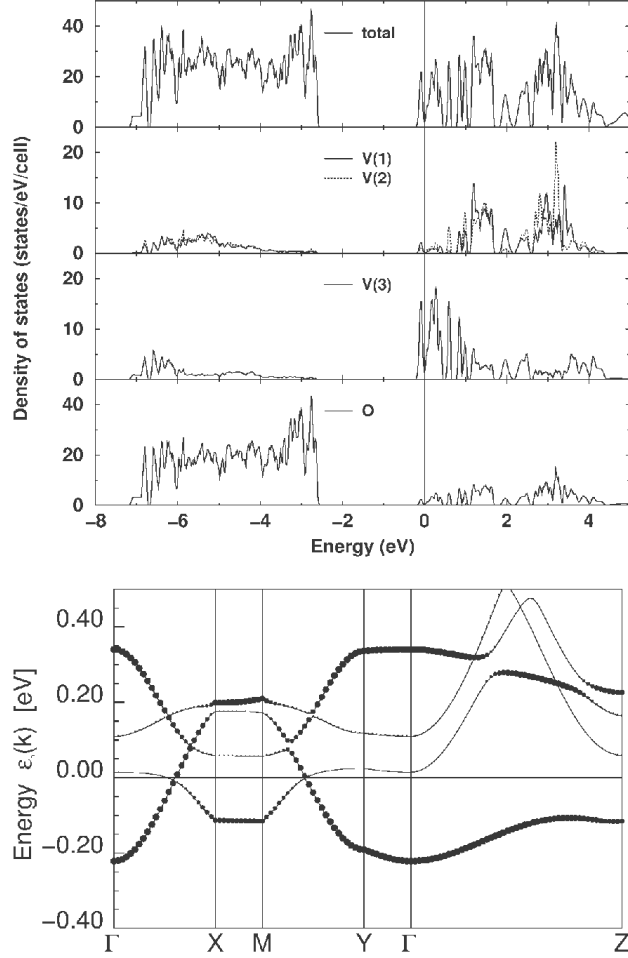


FIG. 8. Upper panel: Total and partial density of states for $\text{Sr}_2\text{V}_3\text{O}_9$. The Fermi level is at zero energy. Lower panel: The corresponding band structure zoomed near the Fermi level. The size of the black circles illustrates the contribution of the local V(3) $3d_{xy}$ orbitals allowing a clear assignment of the two half filled bands. The high symmetry points are noted as follows: Γ (0,0,0), X (1,0,0), M (1,1,0), Y (0,1,0) and Z (0,0,1) in units of $(2\pi/a, 2\pi/b, 2\pi/c)$.

for such very anisotropic scenarios the application of Schulz's quantum spin-chain approach⁴⁰ assuming isotropic interchain interactions J_{\perp} , is limited. Assuming $J_{\perp} = 1/2 (J_b + J_c)$, the Néel temperatures for the quasi 1D-cuprate chains were considerably overestimated in Ref. 53. Most remarkably, an empirical estimate of J_{\perp} in Sr_2CuO_3 in the same work,⁵³ using the experimentally observed Néel temperature, leads to a value for the (isotropic) interchain exchange smaller by a factor of about 2-3 than the theoretical estimate. This is very much in line with the present scenario ($J_{\perp}^{theor} = 1/2 (J_b + J_c) = 5$ K and $J_{\perp}^{emp} = 1.9$ K) and a strong indication that the magnetic coupling in such anisotropic systems deserves further theoretical investigation. Another source of the discrepancy could originate from the remaining structural disorder, which obviously has a strong influence on the ordering temperature (see Tab. II).

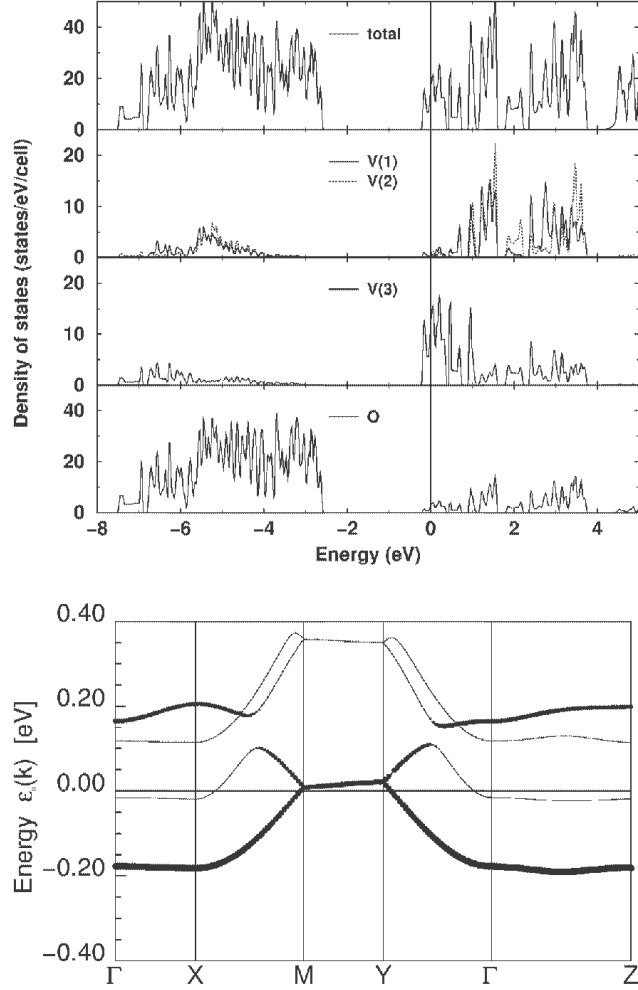


FIG. 9. The same as in Fig.8 but for $\text{Ba}_2\text{V}_3\text{O}_9$.

Now, we turn to the BVO system. In general, the electronic structure of BVO looks rather similar to SVO. The total and the partial DOS as well as the band structure for BVO are shown in Fig. 9. Like in SVO, two vanadium species are clearly distinct, leading to tetrahedrally coordinated nonmagnetic V^{+5} ions (V(1) and V(2)) and a spin $1/2$ V^{+4} ion (V(3)) inside the edge sharing octahedra. In contrast to SVO, the largest dispersion of the bands at the Fermi level along the XM direction (see lower panel in Fig. 9) is parallel to the octahedra chain, confirming the picture from the bond analysis in Section II. A formal TB analysis in terms of NN interactions only like in SVO yields $t_b \sim 90$ meV, $t_a \sim 15$ meV and $t_c \sim 15$ meV. Analogous to the procedure in SVO described above, this results in exchange couplings $J_a \sim 80$ K and $J_b = J_c \sim 2$ K. Again, the largest calculated coupling $J_a = 80$ K is in good agreement with the value of 94 K from the fit to the experimental data. A closer look at the band structure with respect to the interchain couplings (lines ΓX , MY and ΓZ in Fig. 9) shows that an TB analysis in terms of NN only is rather problematic. The strong non cosine-like shape of these dispersions, especially

along ΓZ , is due to contributions from more distant neighbors. The estimate of the corresponding exchange terms and the investigation of the resulting complicated interplay of competing frustrating exchange interactions and their influence on the ordering temperature is far beyond the scope of the present work. Thus, the understanding of the absence of long range order in BVO down to 0.5 K remains an open problem for further work.

It should be noted that in both systems, the crystal field splitting Δ for the $V(3d-t_{2g})$ levels is unusual small in the present band structure calculation compared to other vanadates. This is a possible indication for an enhanced DM interaction (being proportional to $1/\Delta$). A quantitative estimate of the split Δ from our calculation would be problematic due to the known failure of LDA resulting in a metallic solution with the half filled states at the Fermi level instead of an insulating behavior as observed in the experiment. The calculation of Δ , using a more appropriate method, e.g. LDA+ U , is a future task.

VII. SUMMARY

We have investigated the magnetic and the thermodynamic properties of two ternary Vanadium oxide compounds, SVO and BVO, where the magnetic V^{+4} ions are located off-centered in VO_6 octahedra, forming chains. Analysis of the results show that both compounds are quasi one-dimensional spin systems, with *intra-chain* exchanges $J = 82 K$ and $J = 94 K$ for SVO and BVO, respectively. In SVO, antiferromagnetic ordering at $T_N = 5.3 K$ indicate a weak *inter-chain* exchange $J_{\perp} = 1.9 K$. In contrast, no evidence for magnetic order could be observed in BVO, pointing to a very small $J_{\perp} (< 0.15 K)$. The conjecture, based on simple standard arguments, that in SVO the magnetic chain is perpendicular to the structural VO_6 -octahedra chain is confirmed by an analysis of elaborated LDA calculations. Both compounds present an unusual upturn of the susceptibility at low temperatures, which we suggest to be due to a sizeable DM-interaction. In SVO the size of this low temperature upturn as well as the antiferromagnetic ordering temperature increase when the samples are annealed. This peculiar low temperature behaviour shall be the subject of future detailed investigations carried out on single crystals.

¹ M. Hase, I. Terasaki and K. Uchinokura, Phys. Rev. Lett **70**, 3651 (1993).

² M. Hase, J. Magn. Mater. **177 – 181**, 611 (1998) and references therein.

³ K. Fabricius, A. Klümper, Ü. Low, B. Büchner, T. Lorenz, G. Dhaleene and A. Revcolevschi, Phys. Rev. B **57**, 1102 (1998) and references therein.

⁴ I. E. Dzialoshinskii, Sov. Phys. JETP **5**, 1259 (1957).

⁵ T. Moriya, Phys. Rev. **120**, 91 (1960).

⁶ I. Affleck, M. Oshikawa, Phys. Rev. B **60**, 1038 (1999).

⁷ M. Oshikawa, K. Ueda, H. Aoki, A. Ochiai and M. Kohgi, J. Phys. Soc. Jpn. **68**, 3181 (1999).

⁸ R. Feyherm, S. Abens, D. Günther, T. Ishida, M. Meißner, M. Meschke, T. Nogami and M. Steiner, J. Phys.: Condens. Matter **12**, 8495 (2000).

⁹ Y. Ueda, J. Phys. Soc. Jpn. **69** Suppl. B, 149 (2000).

- ¹⁰ Y. Ueda, Chem. Mater **10**, 2653 (1998).
- ¹¹ M. Schindler, F. C. Hawthorne and W. H. Baur, Chem Mater **12**, 1248 (2000) .
- ¹² P. Y. Zavalij and M. S. Whittingham, Acta Cryst. B **55**, 627 (1999).
- ¹³ S. Boudin, A. Guesdon, A. Leclaire and M. M. Borel, Int. J. Inorg. Mat. **2**, 561 (2000).
- ¹⁴ M. A. Korotin, I. S. Elfimov, V. I. Anisimov, M. Troyer and D. I. Khomskii, Phys. Rev. Lett. **83**, 1387 (1999).
- ¹⁵ M. Kanada, H. Harashina, S. Tanaka, T. Fukamachi, Y. Kobayashi and M. Sato, J. Phys. Soc. Jpn. **67**, 2904 (1998).
- ¹⁶ M. Onoda, N. Nishiguchi, J. Solid State Chem. **127**, 359 (1996).
- ¹⁷ H. J. Koo and M. H. Whangbo, Solid State Commun **111**, 353 (1999).
- ¹⁸ G. Liu and J. E. Greedan, J. Solid State Chem. **103**, 139 (1993).
- ¹⁹ M. H. Whangbo, H. J. Koo and K. S. Lee, Solid State Commun **114**, 27 (2000).
- ²⁰ Y. Takeo, T. Yosihama, M. Nishi, K. Nakajima, M. Isobe, Y. Ueda, K. Kodama, H. Harashina, M. Sato, K. Ohoyama, H. Miki and K. Kakurai, J. Phys. Chem. Solids **60**, 1153 (1999).
- ²¹ W. E. Pickett, Phys. Rev. Lett. **79**, 1746 (1997).
- ²² K. Takano and K. Sano, J. Phys. Soc. Jpn. **67**, 4209 (1998).
- ²³ Y. Oka, T. Yao, N. Yamamoto, M. Ueda and S. Maegawa, J. Solid State Chem. **149**, 414 (2000).
- ²⁴ R. V. Shpanchenko, V. V. Chernaya, A. M. Abakumov, E. V. Antipov, J. Hadermann, G. Van tendeloo, E. E. Kaul, C. Geibel, D. Sheptyakov and A. M. Balagurov, Z. Anorg. Allg. Chem. **627**, 2143 (2001).
- ²⁵ M. Isobe and Y. Ueda, J. Phys. Soc. Jpn. **65**, 1178 (1996).
- ²⁶ H. Sawa, E. Ninomiya, T. Ohama, H. Nakao, K. Ohwada, Y. Murakami, Y. Fuji, Y. Noda, M. Isobe and Y. Ueda, J. Phys. Soc. Jpn. **71**, 385 (2002).
- ²⁷ P. Millet, F. Mila, F. C. Zhang, M. Mambrini, A. B. Van Oosten, V. A. Pashchenko, A. Sulpice and A. Stepanov, Phys. Rev. Lett. **83**, 4176 (1999).
- ²⁸ J. L. Gavilano, S. Mushkolaj, H. R. Ott, P. Millet and F. Mila, Phys. Rev. Lett. **85**, 409 (2000).
- ²⁹ F. Mila and F. Zhang, cond-mat/0006068, 5 Jun 2000.
- ³⁰ J.C. Bouloux, J. Galy and P. Hagenmüller, Rev. Chem. Miner. **11**, 48 (1974).
- ³¹ J. Feldmann and Hk. Müller-Buschbaum, Z. Naturforsch. **50b**, 43 (1995).
- ³² J. Feldmann and Hk. Müller-Buschbaum, Z. Naturforsch. **51b**, 489 (1996).
- ³³ O. Mentre, A.C. Dhaussy, F. Abraham, H. Steinfink, J. Solid State Chem. **140**, 417 (1998).
- ³⁴ A.C. Dhaussy, F. Abraham, O. Mentre, H. Steinfink, J. Solid State Chem. **126**, 328 (1996).
- ³⁵ V. Bobnar, P. Lunkenheimer, A. Loidl, E. E. Kaul and C. Geibel, Solid State Commun. **122**, 595 (2002).
- ³⁶ A. Klümper, Eur. Phys. J. B**5**, 677 (1998).
- ³⁷ D. C. Johnston, R. K. Kremer, M. Troyer, X. Wang, A. Klümper, S. L. Bud'ko, A. F. Panchula and P. C. Canfield, Phys. Rev. **B61**, 9558 (2000).
- ³⁸ S. Eggert, I. Affleck and M. Takahashi, Phys. Rev. Lett. **73**, 332 (1994).
- ³⁹ M. Takahashi, Phys Rev **B40**, 2494 (1989).
- ⁴⁰ H. J. Schulz, Phys. Rev. Lett. **77**, 2790 (1996).
- ⁴¹ V. A. Ivanshin and J. Sichelschmidt, unpublished.
- ⁴² D. C. Dender, D. Davidovic, D. H. Reich, C. Broholm, K. Lefmann and G. Aeppli, Phys. Rev. **B53**, 2583 (1996).
- ⁴³ K. Koepfner and H. Eschrig, Phys. Rev. B **59**, 1743 (1999).
- ⁴⁴ J. P. Perdew and A. Zunger, Phys. Rev. B **23**, 5048 (1981).
- ⁴⁵ H. Eschrig, *Optimized LCAO Method and the Electronic Structure of Extended Systems* (Springer, Berlin, 1989).
- ⁴⁶ For the direction of the “structural” chains, a larger ferromagnetic contribution to J can not be excluded, resulting in a somewhat reduced total AFM exchange along this direction.
- ⁴⁷ K. Held, G. Keller, V. Eyert, D. Vollhardt, and V. I. Anisimov, Phys. Rev. Lett. **86**,

- 5345 (2001).
- ⁴⁸ T. Mizokawa, A. Fujimori, Phys. Rev.B **48**, 14150 (1993); J. Zaanen, G. A. Sawatzky, J. Solid State Chem., **88**, 8 (1990).
- ⁴⁹ H. Rosner, R. R. P. Singh, W. H. Zheng, J. Oitmaa, S.-L. Drechsler, and W. E. Pickett, Phys. Rev. Lett. **88**, 186405 (2002); H. Rosner, R. R. P. Singh, W. H. Zheng, J. Oitmaa, and W. E. Pickett, Int. Journ. of Mod. Phys. B, **16**, 1649 (2002).
- ⁵⁰ K. Kojima, M. Larkin, B. Nachumi, Y. Uemura, H. Eisaki, M. Motoyama, S. Uchida, B. Sternlieb, and G. Shirane, Czechoslovak Journal of Phys. **46**, Suppl. S4, 1945 (1996).
- ⁵¹ K. Yamada, J. Wada, S. Hosoya, Y. Endoh, S. Noguchi, S. Kawamata, and K. Okuda, Physica C, **253**, 135 (1995).
- ⁵² K. M. Kojima, Y. Fudamoto, M. Larkin, G. M. Luke, J. Merrin, B. Nachumi, Y. J. Uemura, N. Motoyama, H. Eisaki, S. Uchida, K. Yamada, Y. Endoh, S. Hosoya, B. J. Sternlieb, and G. Shirane, Phys. Rev. Lett. **78**, 1787 (1997).
- ⁵³ H. Rosner, H. Eschrig, R. Hayn, S.-L. Drechsler, and J. Málek, Phys. Rev.B **56**, 3402 (1997)